Int. J. Radiation Oncology Biol. Phys., Vol. 25, pp. 695–701
Printed in the U.S.A. All rights reserved.

0360-3016/93 $6.00 + .00
Copyright © 1993 Pergamon Press Ltd.

● *Therapeutic Oncologic Imaging*

THE EFFECT OF RADIATION ON NORMAL HUMAN CNS AS DETECTED BY NMR SPECTROSCOPY

S. K. SZIGETY, M.SC.,[1] P. S. ALLEN, PH.D.,[1] D. HUYSER-WIERENGA, B.SC.N.[2] AND R. C. URTASUN, M.D.[2]

[1]Department of Applied Sciences in Medicine, University of Alberta, Edmonton, AB; and [2]Department of Radiation Oncology, Cross Cancer Institute, Edmonton, AB

In a prospective study, proton (^{1}H) and phosphorus (^{31}P) nuclear magnetic resonance spectroscopy were used to search for effects of brain tumor radiotherapy on normal human central nervous system. Phosphorus spectroscopy data at 1.5 T seems to suggest that any radiation induced damage that may occur as a result of therapeutic brain irradiation, does not alter the relative concentrations of phosphorus metabolites or the intracellular pH beyond the limits of normal variation (approximately ±20%). Proton spectroscopy, on the other hand, detects post radiation changes in the ratios of certain nuclear magnetic resonance visible metabolites following radiotherapy, particularly choline/N-acetylaspartate, and especially in regions of brain receiving high doses of radiation. Such changes may be indicative of the release of membrane bound choline during radiation induced demyelination of brain. Of interest, we have found elevated metabolite ratios of ^{31}P in normal central nervous system prior to radiotherapy, which persisted throughout the time span of the study in both the ipsilateral and contralateral cerebral hemispheres.

Brain, Central nervous system (CNS), Nuclear magnetic resonance (NMR), Radiation therapy, Radiation effects.

INTRODUCTION

During external beam radiation treatment of brain tumors, radiation exposure to normal tissue that lies within the treatment volume is unavoidable. Delayed effects resulting from this exposure may cause various pathological conditions, including demyelination (4, 5, 13) and radiation necrosis (7, 8). Although these effects may result in the development of clinical symptoms, autopsies of irradiated animal brains have, in fact, shown the presence of radiation-induced damage, in the absence of symptoms (7).

Late injury effects have been observed in magnetic resonance images (MRI) of the human central nervous system following therapeutic radiation (9, 11, 12, 14, 21, 26, 30). The radiation damage appears as high signal regions, particularly in the white matter, on T_2 weighted nuclear magnetic resonance (NMR) images of the brain. However, investigation into the biochemical nature of these alterations has, until recently, been limited to *in vitro* work. The application of NMR spectroscopy has provided a non-invasive diagnostic tool to observe changes in brain and it has the potential to detect radiation induced biochemical changes in irradiated normal brain parenchyma. Previous NMR spectroscopic studies have centered on single dose irradiation of animal brains (7, 8, 11). It is likely that the animal models which receive single dose irradiation may not be representative of the damage caused to human brain by the fractionated doses received during radiotherapy.

The purpose of our study was to observe the changes, detectable by NMR, that occur in human brain following fractionated clinical radiotherapy. Two different nuclear species were used to investigate brain irradiation effects, namely, phosphorus and proton. The application of these techniques to monitor brain tissue in humans non-invasively, allowed actual clinical data to be established, hence removing the degree of uncertainty found in data from animal model studies.

METHODS AND MATERIALS

All experiments were conducted on a 1.5 T. Philips Gyroscan clinical NMR system. Phosphorus spectroscopy was performed to measure alterations in energy metabolism through changes in the high energy phosphate components of the spectrum, while it was hoped that proton spectroscopy might reveal changes in lipid or amino acid metabolism.

Reprint requests to: R. C. Urtasun, M.D., Department of Radiation Oncology, Cross Cancer Institute, 11560 University Ave., Edmonton, Alberta T6G 1Z2 Canada.

Accepted for publication 9 October 1992.

Human subjects

Nuclear magnetic resonance spectra acquired from the group of healthy volunteers allowed us to establish baseline values and normal variations for spectroscopic data. The majority of the control population were examined at only a single time point. However, 2 control volunteers were each studied 10 times over an 8 month period to evaluate the serial variability of ^{31}P spectra. Of the remaining control volunteers, half were analyzed using ^{31}P and half by proton spectroscopy. The second population, the group of patients undergoing radiotherapy for the treatment of their primary brain tumors, was chosen as a model for the study of radiation effects in brain. These two groups of subjects were not age matched. All patients had undergone either tumor biopsies or subtotal resection 2–3 weeks prior to being entered into this study, and the histopathology of the lesions ranged from pituitary adenomas to glioblastomas, with the majority being malignant gliomas (Table 1). Variations in response to radiation because the patients were not examined at the same precise time after surgery were expected to be negligible. The differences between tumor type, another potential source of variability in brain metabolism, were also assumed to give rise to negligible differences in the radiation effect to normal CNS.

Patients were scheduled to receive radiation doses of up to 8000 cGy utilizing either daily or multiple daily fractions with a 6 Mv linear accelerator as the source of high energy x-rays. All patients were entered into this study prior to their radiation treatment, with additional NMR spectroscopy scans scheduled at 0, 2, 4, 8, 12, and 24 months following completion of radiotherapy. A total of 23 patients and 20 healthy volunteers were involved in the study. Only phosphorus spectroscopy was performed during the first part of the study, but patients entering the study at a later date were analyzed using proton spectroscopy. All patients and volunteers signed an informed consent approved by the Institutional Review Board.

Spectroscopy

During each NMR session, spectra were acquired from two regions of brain parenchyma that were not affected by tumor. One region was located in the high dose radiated volume of the brain and the other region was located in part of the contralateral hemisphere exposed to lower doses of radiation. High dose regions in the ipsilateral tumor bearing hemisphere but outside of the tumor and peritumoral edema received 65% (range 50–80) of the total radiation dose, while low dose regions in the contralateral hemisphere received 35% (range 25–50). If possible, anatomically similar lobes of brain were analyzed in opposite hemispheres. The volume of interest was 27 ml, in the case of proton spectroscopy, and slightly larger in the case of phosphorus spectroscopy. Nuclear magnetic resonance images of the brain were used to identify the location of the region of interest in order to ensure that signal from enhancing tumor or peritumoral edema was precluded from both ^{1}H and ^{31}P studies. The head coil was used for imaging the patients analyzed by ^{1}H spectroscopy, while surface coil imaging was performed on patients undergoing ^{31}P spectroscopy. These images also ensured the reproducibility of the locations of the regions of interest in subsequent NMR sessions.

Table 1. Patients entered in study

	^{31}P spectroscopy	^{1}H spectroscopy
Total patients	13	10
Tumor type		
High grade glioma (AAF and glioblastoma)	11	3
Low grade glioma	1	2
Pituitary adenoma	0	3
Oligodendroglioma	1	2

The coil system used for phosphorus spectroscopy was a concentric system, with an outer 6 cm diameter coil being tuned to the phosphorus resonance frequency, while the inner 5.5 cm diameter coil was tuned for protons to facilitate shimming of the region of interest in the brain. The pulse sequence used for ^{31}P spectral acquisition was a depth pulse sequence (2), which removed signal from the high flux bands that are created close to the surface coil, and thus minimized artefactual signal from the surface muscle of the scalp. A sweep width of 3000 Hz was used. Signals from 156 scans were averaged with a repetition interval of 4 sec between each scan, to result in a data acquisition time of 10.4 min. Most of the ^{31}P spectra were acquired using methylene diphosphonic acid (MDA) as an external standard. The MDA was contained in a 1.5 ml sphere placed on the surface coil axis at the location of the 90° tip angle. Similar procedures were performed on the healthy volunteers.

A saddle configuration head coil was used to acquire the proton spectra, using Stimulated Echo Aquisition Mode (STEAM) as the localization technique (10). The critical pulse intervals were TE = 136 milliseconds, TM = 40 milliseconds and TR = 3.0 sec. The averaging of 128 scans resulted in a 6.4 min data acquisition time. Suppression of the water peak, which dominates the proton spectrum of biological systems, was achieved through selective dephasing of the water signal using a Dante pulse (19) prior to the STEAM sequence and by selective inversion of the metabolite peaks using an inversion recovery pulse in the mixing period. Again, similar procedures were used when performing proton spectroscopy on the healthy volunteers.

Data analysis

All spectra were processed with a subtractive baseline correction, two orders of phase correction, and for ^{31}P spectra, a convolution difference using line broadenings of 150 Hz. The spectra were subsequently fitted by a simplex curve fitting routine that approximates each spectral

line independently to a bell shaped curve that was manually chosen to be either a Lorentzian, a Gaussian or a combination of the two. A derivation of the Henderson-Hasselbach equation allowed calculation of intracellular pH of brain from the change in chemical shift of Pi between its basic and dibasic forms, using PCr as the chemical shift standard in the ^{31}P NMR spectrum (23).

RESULTS AND DISCUSSION

Phosphorus spectroscopy

Thirteen patients were entered in the ^{31}P spectroscopy study, and five survived more than 1 year following the end of radiation therapy. The mean survival time for patients with malignant gliomas is 9 months from the time of diagnosis (3). Therefore, tumor recurrence was the most common cause of non-compliance of patients in our study.

Our *in vivo* phosphorus spectra of human brain at 1.5 T allowed the resolution of seven measurable peaks (Fig. 1a). Five of the peaks (gamma ATP, Pi, PCr, PME, and PDE) were observed to sit on a broad background and a calculation of the areas under these peaks prior to concentration ratio estimation, required the use of curve-fitting techniques. Among both patients and healthy volunteers, a considerable variation was detected in the ratio of metabolite peak areas relative to that of total ATP. All metabolite ratios display standard deviations of approximately ±20%, with the exception of PCr, which has less than a 15% deviation (Table 2). Although the greatest

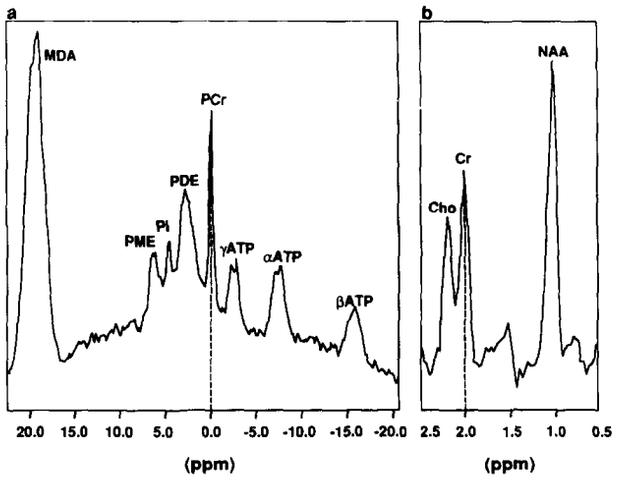

Fig. 1. Typical *in vivo* NMR Spectra from the CNS of healthy volunteers. (a) A typical phosphorus spectrum. The peak at 18 ppm arises from methylene diphosphonic acid, the external standard. The remainder of the NMR peaks arise from brain metabolites: phosphomonoesters (PME), inorganic phosphate (Pi), phosphodiesters (PDE), phosphocreatine (PCr), and the three phosphates of adenosinetriphosphate (ATP). (b) A typical proton spectrum. The peaks arising from brain metabolites include those from N-acetyl groups (NAA), creatine and phosphocreatine (Cr), and from choline (Cho).

Table 2. Metabolite peak area ratios found in the CNS of healthy volunteers

Metabolite ratio	Right hemisphere	Left hemisphere
PME/ATP	0.32 ± 0.06	0.31 ± 0.06
Pi/ATP	0.44 ± 0.09	0.43 ± 0.09
PDE/ATP	1.01 ± 0.20	1.09 ± 0.18
PCr/ATP	0.73 ± 0.06	0.68 ± 0.11
NAA/Cho	2.33 ± 0.42	2.12 ± 0.40
NAA/Cr	2.11 ± 0.39	2.08 ± 0.40
Cr/Cho	1.14 ± 0.28	1.03 ± 0.13

variations were observed when comparing data from several different volunteers, there was still a sizeable variation in peak area ratios (14–21%) found for each of two control volunteers. The coil was repositioned in similar positions for each subsequent NMR scan, as shown by the orientation images. We attribute this variability primarily to measurement uncertainty. For example, if the same spectral file is repeatedly processed, variations of up to ±12% are observed between the successive estimates of peak area. Three manual interventions exist in the processing protocol, namely: phasing, baseline correction and peak fitting, each of which is a source of uncertainty. Slight differences in decision made at each of these interventions give rise to a compounding of the variability. As a result, processing reproducibility is a strong function of the initial signal-to-noise ratio (S/N) of the spectrum. We are not alone in reporting substantial variability. A previously reported NMR study of the normal variation in brain metabolites, as observed by ^{31}P spectroscopy, shows variations in metabolite ratios of up to 30% in healthy volunteers (28). ^{31}P studies on human prostate also show large variability in metabolite ratios. For example, PME/ATP ratios differ by ±20% while the PCr/ATP ratios vary ±25% (17, 28). When analyzing separately the left and right side of the brain in healthy volunteers, there was no significant difference between corresponding metabolite ratios (Table 2).

Figure 2 shows a graphical representation of the ^{31}P data. Statistical analysis of variance (ANOVA) of the ^{31}P data confirmed that there were no significant changes in Pi/ATP or PME/ATP ratios, or pH in brain tumor patients following radiotherapy ($p < 0.05$). pH values remained within the limits of normal variation (7.1 ± .05) as established from our healthy volunteers. There was, however, an increase in PCr/ATP and PDE/ATP ratios over those of healthy volunteers, even though these ratios did not change significantly following radiotherapy. The elevated metabolite ratios were apparent prior to radiotherapy, and persisted throughout the time span of the study in both the ipsilateral (tumor bearing) and contralateral cerebral hemispheres.

The elevated PCr/ATP and PDE/ATP ratios observed in the brain tumor patients, as compared to the healthy volunteers, suggested some inherent difference between the two study groups. Residual tumor present in the ip-

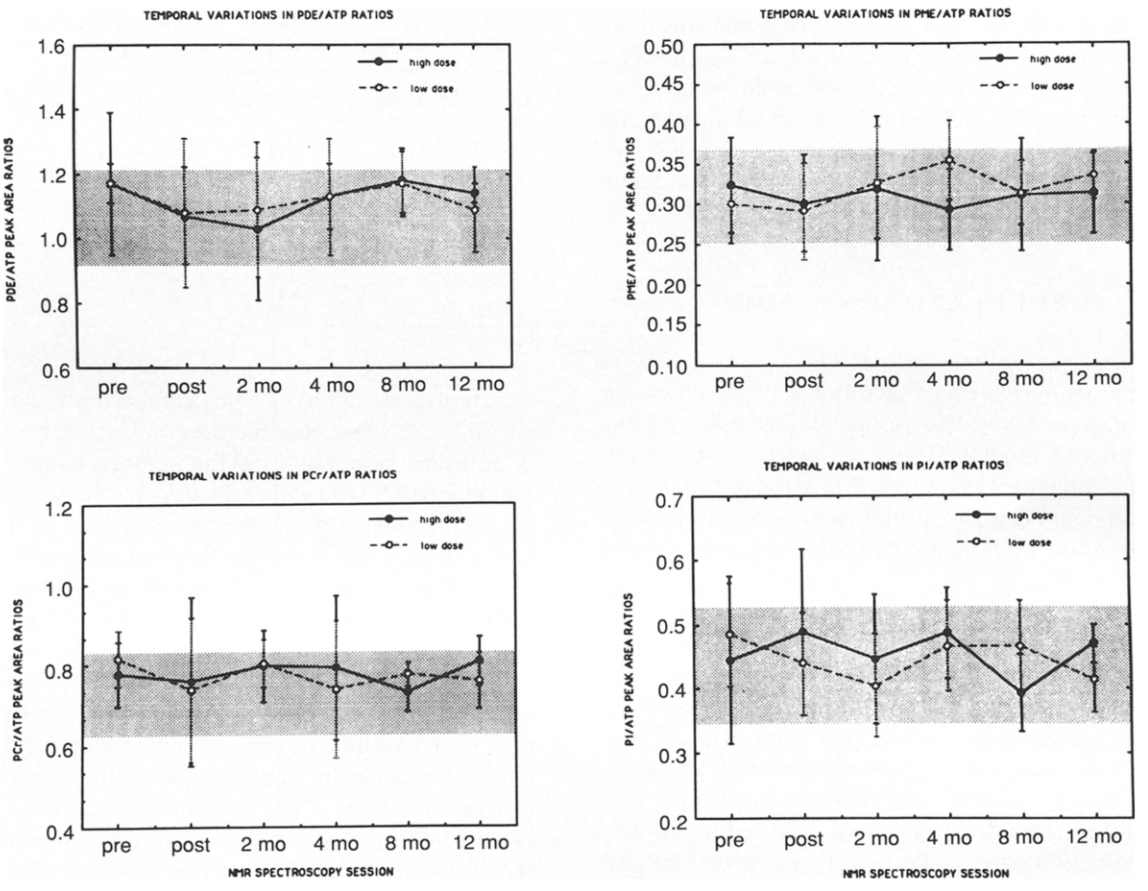

Fig. 2. Metabolite peak area ratios from ^{31}P spectra of non-tumoral CNS tissue in brain tumor patients. The shaded area on each graph represents the range of metabolite ratios found in the normal CNS of healthy volunteers. Error bars represent the standard deviation of values. The numbers of patients analyzed at the pre RT, 0, 2, 4, 8, and 12 month periods are 13, 11, 9, 5, and 5, respectively.

silateral hemisphere, or the effects of previous brain surgery, are unlikely to be the source of these differences, since the "abnormal" ratios were found in both hemispheres of the brain, and the above mentioned conditions exert a more local effect. The first examination was done at least with a minimum of 2 weeks and more often up to four weeks post-surgery and this is generally considered enough time elapsed for the surrounding normal brain to recover from the traumatic surgery. In addition, because of the large tumor volume, it is possible that varying amounts of white/grey matter, away from the tumor, was included in the observed volume and could account as a potential source of variability. We have not attempted to quantify normal grey and white matter differences. In addition, we cannot be absolutely certain that the presence of tumor is not having an effect on CNS metabolism in the whole brain. Radiotherapy was also ruled out as the cause of the higher metabolite ratios, since they were present even prior to RT. However, when comparing data from patients with that from healthy volunteers, one must also consider the age difference between the two groups; our healthy volunteers ranged in age from 20–29 (mean age 26 years) while our patients ranged in age from 24–55 years (mean age 37 years). Our inability to recruit older volunteers thwarted attempts to age match them with patients. Little data is available on the effect that aging has on phosphorus compounds in brain, although gerontological studies on human muscle may yield clues to biochemical changes in brain. In the skeletal muscle of older volunteers, increased PDE levels have been observed (18, 27). Studies on human gastrocnemius muscle have also suggested a decrease in ATP levels with age (27). Studies in aged rat brains have displayed increased methylation of phosphodiesters, suggesting that altered phospholipid metabolism may occur with age (6). Aging might therefore account for the observation of elevated metabolite ratios in the brains of patients. The increase in the PDE/ATP and PCr/ATP ratios are likely due to a combined decrease in ATP levels and the increase in the concentrations of PDE and PCr. Although no evidence was found in the literature to support the increased PCr levels, the relatively unchanged Pi/ATP and PME/ATP ratios between healthy volunteers and the patients, suggests that decreased ATP levels alone may not be sufficient to cause metabolite ratios from the patients to extend beyond the range of normal variation established by our healthy volunteers.

Proton spectroscopy

A total of 10 patients were entered into the proton spectroscopy study. Three distinct and reproducible metabolite peaks were observed in the proton spectrum. These three peaks were the resonances from the methyl protons of choline (Cho), of creatine and phosphocreatine (Cr) and of N-acetyl aspartate (NAA) and related acetyl compounds (Fig. 1b). The resolution of all three peaks was, in the majority of cases, complete, although slight overlap of the choline and creatine peaks was sometimes observed.

Since the localization method of the STEAM pulse sequence prevented the inclusion of an external concentration standard in the field of view all possible metabolite ratios (NAA/Cr, Cr/Cho and NAA/Cho) were therefore compared. The normal variation for each metabolite ratio, as observed from spectroscopic data from our healthy volunteers (Table 2) were about 20%.

Certain metabolite ratios in the CNS of patients, prior to RT, differed from similar ratios in the brains of healthy volunteers. Specifically, NAA/Cr ratios were 78%, and Cr/Cho ratios were 124%, of the "normal" values established from the healthy volunteers. These differences were noted in both the high and the low dose volumes of patient's normal brain. There was no noticeable difference in the NAA/Cho ratio between patients and healthy volunteers prior to RT. This discrepancy may arise from the creatine component of the NAA/Cr and Cr/Cho ratios, because creatine levels in the CSF have been shown to increase with age (1), and because the age difference between the healthy volunteers (26 ± 3 years) and the patients (40 ± 11 years) is 14 years between the means. There were also observable alterations in the ^{1}H NMR spectrum of the CNS of several, though not all, patients following radiotherapy, specifically, marked increases in the choline levels or post-irradiation decreases in Cr/Cho and NAA/Cho ratios, particularly in high dose volumes. These alterations are reflected in the means plotted in Figure 3.

From this information, we postulate that choline levels increase following radiotherapy, but NAA and creatine levels remain relatively unchanged.

The increase in the choline signal that we see in brain following RT, could stem from an increase in the mobility of choline moeties arising from the lipid sources, which in turn may a reflect breakdown of the plasma or intracellular membranes. For example, choline, as a constituent of phosphatidylcholine found in membranous structures of the brain, is largely immobile, having a short transverse relaxation time that renders it NMR invisible with long echo times. This hypothesis is supported by results from a previous study of aqueous brain extracts from rats that had been irradiated *in vivo* (25). In that study, it was reported that decreased NAA/Cho ratios (1.4 ± 0.4, compared to the normal value of 2.0 ± .02) occurred in brain following irradiation. In addition, analysis of organic extracts from the same brains suggested that decreases in phosphatidylcholine, phosphatidlyethanol-

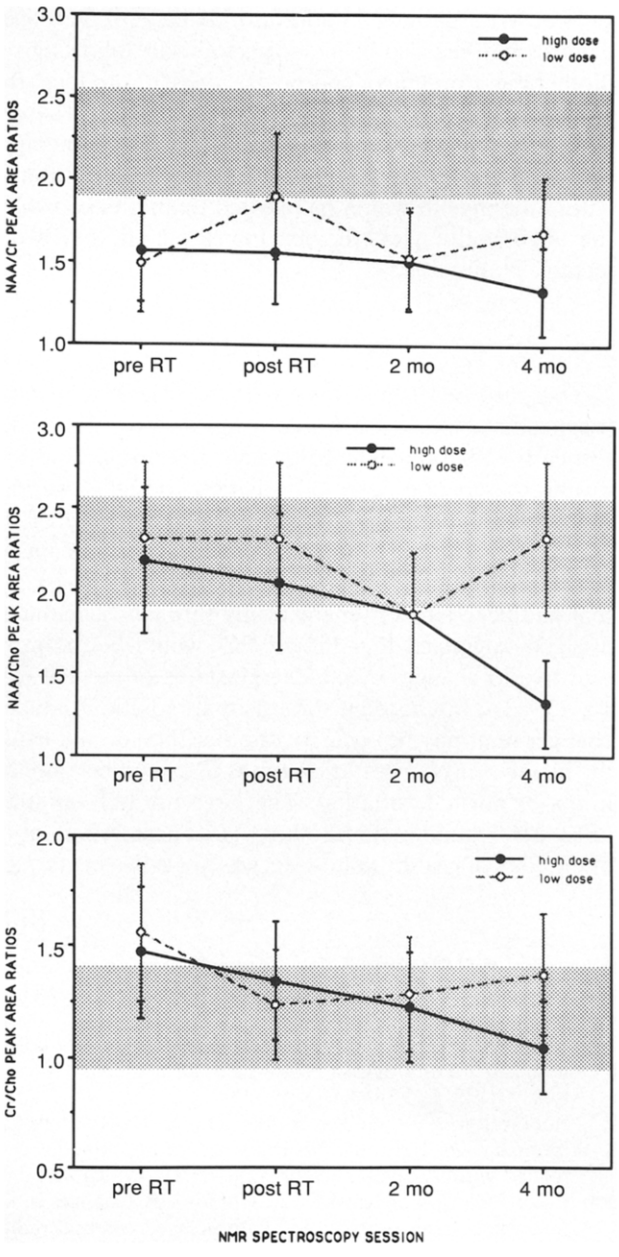

Fig. 3. Metabolite peak area ratios from ^{1}H spectra of non-tumoral CNS tissue in brain tumor patients. The above graphs show temporal changes in metabolite ratios of irradiated brain. The metabolite ratios studied are NAA/Cr (a), NAA/Cho (b), and Cr/Cho (c). The shaded area on each graph represents the normal range of metabolite ratios which are found in the CNS of healthy volunteers. Standard deviations are indicated by the error bars, and the number of patients analyzed at pre RT, 0, 2, and 4 month periods are 4, 6, 3, and 3, respectively.

amine and phosphatidylserine occur. The authors concluded that radiation induced damage to cells may cause the breakdown of membrane lipids, resulting in elevated levels of the water soluble, and therefore mobile, phosphocholine. In this rat study, the Cho levels are again compared to those of the NAA peak, making it difficult to discriminate between changes in choline and changes

in N-acetyl aspartate. In addition, damage to the oligodendrocytes has also been shown to occur following radiotherapy (5). Oligodendrocytes, which produce the choline-rich myelin sheath that surrounds neuronal axons, are shown to decrease in number following radiotherapy. One can therefore postulate that the choline stores found within the myelin would be released upon breakdown of the oligodendrocytes, thereby increasing the NMR-detectable choline signal.

CONCLUSION

The purpose of this study is to determine if nuclear magnetic resonance spectroscopy has the potential to detect early radiation-induced damage in normal CNS following therapeutic doses of radiation. Initially, we had thought that changes in the energy metabolites (PCr, Pi and ATP) would be sensitive to radiation-induced damage to brain. Previous ^{31}P spectroscopic work on normal CNS that had been stressed energetically through ischemia or hypoxia, suggested that Pi and PCr would be the most sensitive to changes in the energy status of the cell (15, 16, 20, 22, 23). Our data suggests that radiation induced changes that may be occurring in the CNS, do not cause the metabolite concentration ratios to extend beyond the limits of normal variation. The large normal variation (±13–21%) found in metabolite/ATP concentration ratios of the CNS of healthy volunteers was not expected, though it is not unique. It originates not only from biological variations, but also from processing reproducibility and measurement uncertainty. Improvements in hardware and technique may be able to reduce the apparent normal variation in phosphorus metabolite concentration ratios from acceptable volumes of brain.

In contrast, the proton spectroscopic data of normal CNS from 10 patients with brain tumors appears to indicate that there are NMR detectable post-radiation changes in regions of brain receiving radiation, particularly the high dose regions and particularly the concentration ratios involving choline. These changes are thought to result from radiation damage to membranes producing soluble phosphocholines. That these phosphomonoesters are not detected in the ^{31}P spectrum is probably a reflection of the relative sensitivities of ^{31}P and ^{1}H spectroscopy.

Because of the very long examination time that it necessitated (3 hr), the two nuclei were not studied in the same patient. The study design concentrated first on one nucleus, ^{31}P, to maximize patient accrual, before turning to the other, ^{1}H. By the time that proton spectroscopy was being undertaken, the majority of patients in the first group had either died or were in too poor a neurological condition to go through the second set of investigations.

Although many of our results are preliminary, the conclusions that we have drawn from this study may form a basis for an eventual use of this technique to detect early radiation induced changes in normal CNS.

REFERENCES

1. Agren, H.; Niklasson, F. Creatinine and creatine in the CSF: indices of brain energy metabolism in depression. J. Neural Transmission 74:55–59;1988.
2. Bendall, M. R.; Gordon, R. E. Depth and refocusing pulses designed for multipulse NMR with surface coils. J. Mag. Res. 53:365–385;1983.
3. Bookwalter, J. W.; Selker, R. G.; Schiffer, L.; Randall, M.; Iannuzzi, D.; Kristofik, M. Brain tumor cell kinetics correlated with survival. J. Neurosurg. 65:795–798;1986.
4. Brock, M.; Cervos-Navarro, J.; Holdorff, B. Changes in intracranial pressure associated with delayed cerebral radionecrosis. Med. Phys. 14:1–37;1984.
5. Burger, P. C.; Mahaley, S.; Dudka, L.; Vogel, F. S. The morphologic effects of radiation administered therapeutically for intracranial gliomas. Cancer 44:1256–1272;1979.
6. Calderini, G.; Toffano, G. Phospholipid methylation. In: Giacobini, E., Filogamo, G., Giacobini, E., Vernadakis, A., eds. The ageing brain. NY: Raven Press; 15–45;1982.
7. Caveness, W. F. Experimental observations: Delayed radiation necrosis in normal monkey brain. In: Gilbert, H. A., Kagan, A. R., eds. Radiation damage to the nervous system. New York: Raven Press; 1–39;1980.
8. Courville, C. B.; Myers, R. O. The process of demyelination in the central nervous system II. Exp. Neurol. 17:158–173;1958.
9. Dooms, G. C.; Hecht, S.; Brant-Zawadski, M.; Berthiaume, Y.; Norman, D.; Newton, T. H. Brain radiation lesions: MR imaging. Radiology 158:149–155;1986.
10. Frahm, J.; Merboldt, K. D.; Hanicke, W. Localized proton spectroscopy using stimulated echoes. J. Magn. Reson. 72: 502–508;1987.
11. Grossman, R. I.; Leavitt, C. M.; Evans, S. M.; Lenkinski, R. E.; Holland, G. A.; Van Winkle, T. J.; McGrath, J. T.; Curran, W. J.; Shetty, A.; Joseph, P. M. Experimental radiation injury. Radiology 169:305–309;1988.
12. Hecht-Leavitt, C.; Grossman, R. I.; Curran, W. J.; McGrath, J. T.; Biery, D. N.; Joseph, P. M.; Nelson, D. F. MR of brain radiation injury. AJNR 8:427–430;1987.
13. Heindel, W.; Bunke, J.; Steinbrich, W.; Friedman, G. Human brain tumors (Abstr.). Proceedings from the 6th SMRM, New York; 1987.
14. Hoffman, W. F.; Levine, V. A.; Wilson, C. B. Evaluation of malignant glioma patients during the postirradiation period. J. Neurosurg. 50:624–628;1979.
15. Hope, P. L.; Cady, E. B.; Chu, A.; Delpy, D. T.; Gardiner, R. M.; Reynolds, E. O. R. Brain metabolism and intracellular pH during ischemia and hypoxia. J. Neurochem. 49: 75–82;1987.
16. Komatsumoto, S.; Nioka, S.; Greenberg, J. H.; Yoshizaki, K.; Subramanian, V. H.; Chance, B.; Revich, M. Cerebral energy metabolism measured *in vivo* by 31-P NMR in middle cerebral artery occlusion in the cat. J. Cereb. Blood Flow Met. 7:557–562;1987.
17. Koutcher, J. A.; Okunieff, P.; Neuringer, L.; Suit, H.; Brady, T. Size dependant changes in tumor phosphate metabolism after radiation therapy as detected by ^{31}P spectroscopy. Int. J. Radiation Oncology Biol. Phys. 13:1851–1855;1987.
18. Moeller, P.; Bergstrom, J.; Furst, P.; Hellstrom, K. Effects of ageing on energy rich phosphagens in human skeletal muscles. Clin. Sci. 58:553–555;1980.
19. Morris, G. A.; Freeman, R. Selective excitation in Fourier transform nuclear magnetic resonance. J. Mag. Res. 29:433–462;1978.
20. Naritomi, H.; Sasaki, M.; Kanashiro, M.; Kitani, M.; Sa-

wada, T. Flow thresholds for cerebral energy disturbances. J. Cereb. Blood Flow Met. 8:16–23;1988.
21. Packer, R. J.; Zimmerman, R. A.; Bilaniuk, L. T. Magnetic resonance imaging in the evaluation of treatment related central nervous system damage. Cancer 58:635–640;1986.
22. Peeling, J.; Sutherland, G. R.; Girvin, J. 1-H NMR analysis of metabolite levels in human epeileptic tissue and brain tumors (Abstr.). Proceedings from the 8th SMRM, Amsterdam; 1989:296.
23. Petroff, O. A. C.; Pritchard, J. W.; Behar, K. L.; Alger, J. R.; den Hollander, J. A.; Schulman, R. G. Cerebral intracellular pH by ^{31}P nuclear magnetic resonance spectroscopy. Neurology 35:781–788;1985.
24. Prichard, J. W.; Alger, J. R.; Behar, K. L.; Petroff, O. A. C.; Shulman, R. G. Cerebral metabolic studies *in vivo* by 31-p NMR. Proc. Natl. Acad. Sci. USA. 80:2748–2751;1983.
25. Richards, T.; Budinger, T. F. NMR imaging and spectroscopy of the mammalian central nervous system after heavy ion radiation. Rad. Res. 113:79–101;1988.
26. Rubin, P.; Whitaker, J. N.; Ceckler, T. L.; Nelson, D.; Gregory, P. K.; Baggs, R. B.; Constine, L. S.; Herman, P. K. Myelin basic protein and magnetic resonance imaging for diagnostic radiation myelopathy. Int. J. Radiat. Oncol. Biol. Phys. 15:1371–1381;1988.
27. Satrustegui, J.; Berkowitz, H.; Boden, B.; Donlen, E.; McLaughlin, A.; Maris, J.; Warnell, R.; Chance, B. An *in vivo* phosphorus NMR study of variations with age on the phosphodiester content in human muscle. Mechan. Aging Devel. 42:105–114;1988.
28. Smith, M. A.; Porter, D.; Lowry, M.; Ayton, V. T.; Richards, M. A.; Twelves, C. J.; Garlick, P.; Maisey, M. N. Precision and normal variations of volume selected *in vivo* spectroscopy (Abstr.). Proceedings from the 7th SMRM, San Francisco; 1988:343.
29. Thomas, M. A.; Kurhanewicz, J.; Jajodia, P.; Karczmar, G.; Hubesch, B.; Matson, G. B.; James, T. L.; Narayan, P.; Weiner, M. W. 31-P NMR spectroscopy of human prostate *in vivo* (Abstr.). Proceedings from the 8th SMRM, Amsterdam; 1989:297.
30. Tsuruda, J. S.; Kortman, K. E.; Bradley, W. G.; Wheeler, D. C.; Dalsem, W. V.; Bradley, T. P. Radiation effects on cerebral white matter. AJN 149:165–171;1987.